parameters of the Gent model. The compression breast thickness at a given compression force is roughly equal for both paddles.

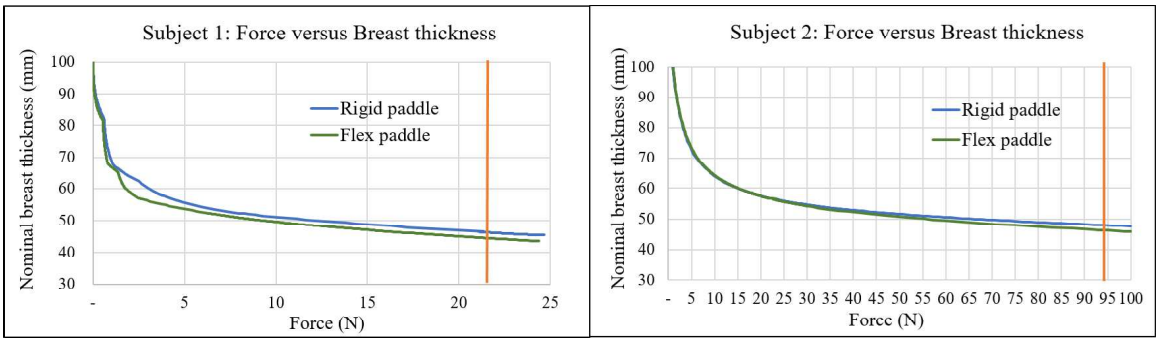

Figure 5.4: Resulting breast flatenning curve as function of the compression force with Gent contitutive model.

5.2 Simulation of digital images

Digital mammographyc images of the compressed breast were simulated using the CatSim simulation environment (de Carvalho, 2014). The X-rays projections of phantom objects were simulated using a GE Senographe Pristina-like system topology (Figure 5.5).

5.2.1 Breast phantom objects

The phantoms were created by first extracting the compressed breast other shape. Then, a set of microcalcifications were inserted into each compressed breast volume. The smallest breast volume contains 21 microcalcifications arranged in a matrix of 7 rows and 3 columns (Figure 5.6.a). The largest breast volume contains 56 microcalcifications arranged in a matrix of 7 rows and 8 columns. The matrix of calcifications is parallel with the entrance surface of the image receptor and positioned at the breast mid thickness (Figure 5.6.b). The distance between two consecutive columns or rows is equal to 10mm. The anatomical background was assumed to be a uniform breast-equivalent material composed of glandular/adipose tissue with a 20/80 ratio. Two simulations were performed for each compression considering $\mu calc$ of 0.2 mm and 0.3mm in diameter.

Microcalcifications ($\mu calc$) were simulated as round-shaped surface mesh. To add irregularities and randomness, initially spherical objects were randomly deformed . The deformation consisted of two steps. First, the sphere surface was slightly deformed to a random ellipsoid along three randomly chosen axes, with maximum deformation magnitude set to five percent of the $\mu calc$ diameter. Then the surface meshes were modified according to a stochastic Perlin noise to create irregularities. The Perlin noise deformation was done by locally displacing the vertices of a surface mesh in directions perpendicular to the mesh face. The displacement magnitude was set to $20\mu m$.

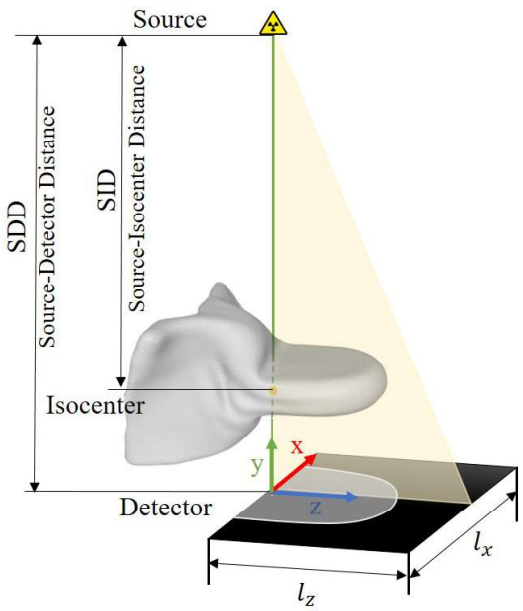

Figure 5.5: A schematic illustration og the simulated GE Senographe Pristina TM mammography unit.

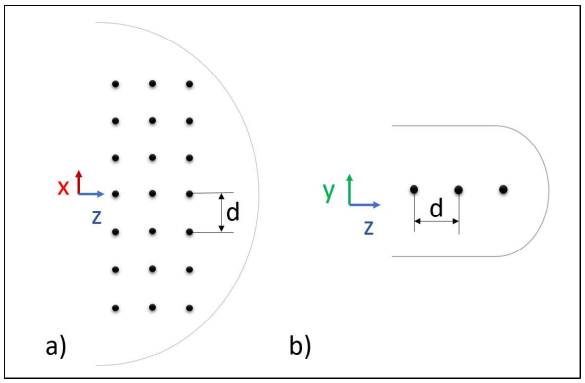

Figure 5.6: Microclcification distribution over the smallest breast volume ($d = 10mm$): a)axial view, b) sagittal view.

Microcalcifications with x-ray attenuation properties corresponding to the attenuation of aluminum (Al) at 24 keV and with a volumetric mass density corresponding to 60% of the Al density, i.e. 1.63 kgm^3, were designed. The choice of 24 keV corresponded to the photon energy of the x-ray source used in our study. Al is less attenuating than the minerals composing real $\mu calc$ which contain calcium carbonate, calcium oxalate or apatite. This is realistic since in real ($\mu calc$), the minerals are embedded in a protein matrix; therefore the attenuation of a ($\mu calc$) is lower than when considering only the minerals.

5.2.2 Physical characteristics

Physical characteristics of the imaging system were modeled as follows. A simplified monoenergetic x-ray source was used. The photon energy level was set to 24 keV, this is equivalent to the effective x-ray energy of a 34 kVp Rhodium (Rh)/Silver (Ag) target/filter spectrum used for imaging a 46 mm compressed breast. An ideal point source focal-spot was used. In order to simulate the detector unsharpness, a modulation transfer function empirically measured from the reference system was used by the simulator. X-ray scatter from the test object was not considered. Only Poisson x-ray noise was added and the electronic noise was not modeled.

A calibration was performed to match the signal-to-noise ratio (SNR) in simulated images with the SNR obtained in experimentally acquired images using the GE Senographe Pristina system with automatic optimization of parameters. The adjustment method is described as follows. On the GE Senographe Pristina system, FFDM central raw projection images were acquired from 2 phantoms (CIRS, Virginia, USA) with 100% adipose and 100% fibroglandular equivalent composition. The phantoms were positioned side-by-side on the breast positioning table. The acquisitions were repeated for five different breast thicknesses $\{45, 50, 60, 65, 70\ (mm)\}$. Images of the $45mm$ thick phantom was acquired at 26 kVp, the images of the others four phantoms were acquired at 34 kVp. A Rh/Ag target/filter combination was used with the AOP mode. SNR values were measured in the raw projection images (processed only with the manufacturers gain, offset, and defective pixel correction), in $2cm \times 2cm$ square ROIs at 5 cm from the chest wall. SNR was defined as $\frac{\langle SI \rangle}{\sigma_{SI}}$, where $\langle SI \rangle$ is the average detected signal intensity per pixel and σ_{SI} is the standard deviation in the signal intensity. The corresponding experiments was then simulated. The mAs value in the simulation was adjusted so as SNR values in the simulated and experimentally obtained images were found similar. Due to restrictions of the x-ray simulator, it was not possible to exactly match the SNR for both 100% adipose and 100% fibroglandular regions. The mAs in the simulations was therefore adjusted till SNR differed by maximum 10% in both breast-tissue equivalent.

5.3 Compression quality metrics

The measures used to quantify the three criteria characterizing the quality of breast compression (patient comfort, image quality and average glandular dose) are described in the following section.

5.3.1 Patient comfort

Today, the pain estimation and quantification still remains an open question. During mammography, the perceived pain, or it's interpretation, may depend on the social status, pain history or psychological condition of the patient. But can also depend on the physical parameters as the compression force, amount of deformation or pressure on the skin surface.